Available online at www.sciencedirect.com
ScienceDirect
Journal of Molecular Spectroscopy 241 (2007) 124–135
Journal of MOLECULAR SPECTROSCOPY
www.elsevier.com/locate/jms

Microwave study of the submillimeter spectrum of the $H_2O\cdots HF$ dimer

S.P. Belov, V.M. Demkin, N.F. Zobov, E.N. Karyakin, A.F. Krupnov, I.N. Kozin, O.L. Polyansky, M.Yu. Tretyakov *

Institute of Applied Physics of RAS, 46 Uljanova street, 603950 Nizhny Novgorod, Russia

Received 9 June 2006; in revised form 21 November 2006
Available online 16 December 2006

Abstract

The study of the rotational spectrum of the $H_2O\cdots HF$ dimer in the equilibrium gas phase in the range 180–350 GHz by continuously frequency scanning microwave spectrometer with backward-wave oscillator and acoustic detection of absorption is described. The results of analyzing of the most intense spectral series are given. The assignment of some spectral series observed earlier is corrected. Data on the Coriolis interaction between the ground and excited vibrational states are obtained and spectroscopic constants of the dimer are significantly refined.

Keywords: $H_2O\cdots HF$ dimer; Equilibrium gas phase; Millimeter–submillimeter wavelengths; Experimental spectrum analysis; RAD-3 spectrometer

1. Preface

The molecular complex $H_2O\cdots HF$ is a potentially very interesting system. First, it is one of the very few complexes (among them $HF\cdots HF$ dimer, [6,7]) whose spectra can be observed in the gaseous equilibrium phase. This opens the way to observe highly excited intermolecular low energy modes and to characterize experimentally much more extensive areas of the potential energy surface than it is possible for the huge number of molecular complexes, mostly of the Van-der-Waals type, observed in beams and jets. Second, its electronic structure is close to that of water dimer and $H_2O\cdots HF$ dimer could serve as a simpler prototype for water dimer investigations.

We did the work presented in this paper about 18 years ago and published it in the form of a preprint in Russian. We think that it would be good for the spectroscopic community if we publish it now in the form available for the general audience. We feel that it makes sense to publish a translation of our original preprint without updating it, because the main features of the work remain the same. However we present references [29–33] to the most recent work on this molecular complex, which shows the growing interest in this complex from both theoretical and experimental points of view. In particular, from Ref. [33] it is clear that modern *ab-initio* theory is much more capable of working with $H_2O\cdots HF$ complex. It gives hope that full dimensional calculations of the potential energy and energy levels of this dimer are becoming more and more realistic [34].

2. Introduction

Investigations of molecular complexes are of great interest from the viewpoint of studying qualitative characteristics of the hydrogen bond as well as intermolecular interactions. The relative weakness of the bond between monomers in the complex leads to large amplitude motions including anomalous centrifugal distortions, inversions and low-frequency vibrations. All of these characteristics of complexes can be precisely studied by the methods of high resolution molecular spectroscopy in the gas phase. The biggest and the most intense part of the rotational spectra of complexes, including the transitions with high rotational

* Corresponding author. Fax: +7 8312 36 37 92.
E-mail address: trt@appl.sci-nnov.ru (M.Yu. Tretyakov).
URL: http://www.mwl.sci-nnov.ru/ (M.Yu. Tretyakov).

0022-2852/$ - see front matter © 2006 Elsevier Inc. All rights reserved.
doi:10.1016/j.jms.2006.11.008

quantum numbers J and K (which are of great importance for determining the characteristics of the non-rigidity of the bond) as well as low-frequency vibration-rotational and inversion-rotational spectra of complexes, which characterize the peculiarities of large amplitude motions, fall mainly within the submillimeter and far infrared regions of the spectrum. Experimental studies of spectra of molecular complexes in radio-frequency and centimeter wavelength ranges were started in the seventies in cooled supersonic beams by the team of Klemperer at Harvard University and in the equilibrium gas phase by the team of Millen from University College of London (see for example reviews [1–4]). However more efficient due to aforementioned reasons were studies of molecular complexes at shorter wavelengths and especially in the equilibrium gas phase, when energy levels with high rotational quantum numbers J and K of excited vibrational states of complexes could be populated. Among the most advanced investigators was the team of the National Institute of Standards and Technology of the USA, which studied in 1987 the spectrum of the HF···HF dimmer in the equilibrium gas phase up to frequencies of about 126 GHz [5]. Our studies of the HF···HF dimmer in the equilibrium gas phase [6,7] in the frequency range up to 350 GHz demonstrated the essential advantages of using a RAD spectrometer [8] for such investigations.

The present paper describes the investigation of the submillimeter-wave spectrum of the $H_2O\cdots HF$ dimer.

The microwave spectrum of the hydrogen-bonded heterodimer formed between water and hydrogen fluoride was first observed by Bevan et al. [9]. In two later papers [10,11] the structure of the heterodimer and frequencies of three lowest vibration modes were determined. The heterodimer has a non-planar equilibrium geometry with an out-of-plane angle of ~45°. Water molecule acts in the complex as a proton acceptor and hydrogen fluoride acts as a donor. As follows from the structure the heterodimer is slightly asymmetric rotor with dipole moment oriented practically along the a-axis of the molecule. Because of that a-type of transitions are dominant in its rotational spectrum.

The study of $H_2O\cdots HF$ rotational spectra in the ground and in three lowest vibrational states in the frequency range up to 75 GHz was reported in [12]. Our study widens this range by more than a factor of 4 and extends observations to the region of higher quantum numbers J of the dimer transition sequences which have been already observed in [12] as well as a number of new spectral line series. The present paper describes the experiment and gives the analysis of the most intense spectral series.

3. Experiment

A block-diagram of the RAD-3 spectrometer [13] used for this study is presented in Fig. 1. The radiation source in the spectrometer is a backward wave oscillator (BWO) stabilized against a tunable Fabry–Perot cavity. The $H_2O\cdots HF$ dimer spectrum was observed in the cooled static pressure gas cell with a microphone (RAD-cell) at pressures between 0.3 and 1 Torr and at temperatures ~250 K. The frequency measurements in the spectrometer were performed against the lines of SO_2 reference spectrum [14]. Mean square value of the uncertainty of frequency measurement with RAD-3 spectrometer was determined in preliminary tests as 0.5 MHz for strong isolated lines of monomers. The uncertainty was somewhat larger in the case of weak and broad (~40 MHz) lines of the $H_2O\cdots HF$ dimer having very dense spectrum. However, we consider a value of 3–5 MHz as reasonable estimation of possible error in frequency measurements for most of lines. More detailed description of the RAD-3 spectrometer and analysis of frequency measurement accuracy are given in the appendix.

HF vapor was obtained by thermal decomposition of KFHF according to the procedure described in [15]. The composition of the HF/H_2O gas mixture into the RAD cell was regulated by adding water vapor from a separate flask. The cell (like it had been in [6,7]) was made of stainless steel. Before the experiment the cell was filled with HF vapor and kept for a few hours; this procedure allowed to keep relatively stable condition of the gas mixture during the course of the experiment.

Fig. 2 presents a fraction of the observed spectrum of the $H_2O\cdots HF$ dimer (upper trace) recorded simultaneously with the SO_2 reference spectrum (lower trace). Measured frequencies of the studied $H_2O\cdots HF$ spectrum and tabulated frequencies of the reference SO_2 spectrum [14] are shown next to the lines. Besides the lines in the ground and the first excited vibrational states of the $H_2O\cdots HF$ dimer, one can also find in the Fig. 2 many spectral lines of smaller intensity, belonging to higher excited vibrational states and, perhaps, to another conformer of the dimer. In total we have measured frequencies of several hundred spectral lines of $H_2O\cdots HF$ in the range from 180 to 350 GHz. The analysis of a part of the observed lines is given in the next section.

4. Spectrum analysis

The recorded spectrum contains the pure rotational transitions of $H_2O\cdots HF$ dimer with $\Delta K = 0$ and rotational quantum numbers J ranging from 12 to 25. The low frequency transitions with quantum numbers $J \leqslant 4$ and $K_a \leqslant 3$ were observed earlier [12] for (000), (100), (010) and (001)[1] vibrational states. We have observed the extension of all spectral series, studied in [12], to high values of

[1] Among nine vibrational modes of the complex, only three intermolecular modes are low-frequency ones—smaller than 200 cm^{-1}. They are: a bending mode outside the plane of the dimer 64(10)cm^{-1} ($\upsilon_{\beta(o)}$), a bending mode in the plane of the dimer 157(10) cm^{-1} ($\upsilon_{\beta(i)}$) and the mode corresponding to the stretching of the complex 175(10) cm^{-1} (υ_{σ}) [12]. Taking this into account we shall designate the identification of vibrational states in the form ($\upsilon_{\beta(o)}$, $\upsilon_{\beta(i)}$, υ_{σ}), assuming that quantum numbers of higher frequency modes are always equal to zero.

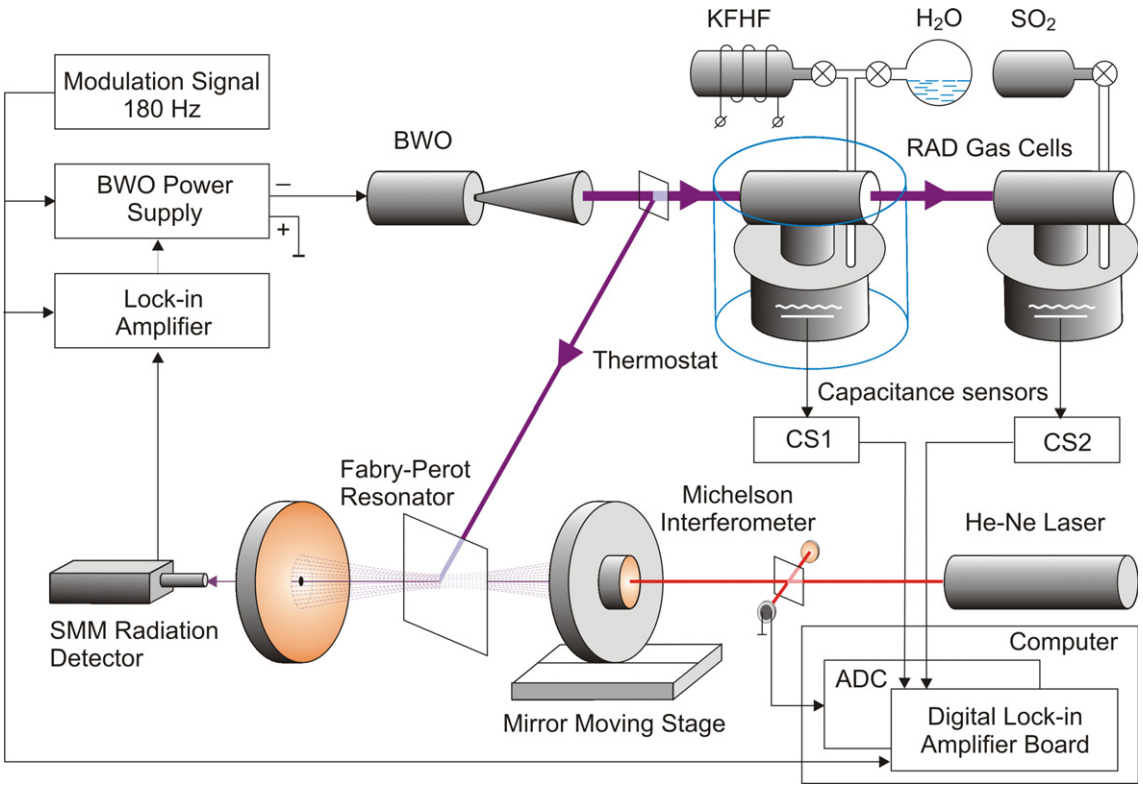

Fig. 1. Block-diagram of the RAD-3 spectrometer. Most essential parts of the spectrometer including BWO, gas cells with related vacuum parts, elements of the resonator and the interferometer fed by the HeNe laser are drawn as they roughly look in reality. Electronic devices are shown schematically.

the rotational quantum numbers J, i.e. the branches of the $H_2O\cdots HF$ rotational transitions with quantum numbers $K_a = 0$, 1, 2 and 3 in the ground (000) state, with $K_a = 0$, 1, 2 and 3 in the (100) state, with $K_a = 0$, 1 and 2 in the (010) state and with $K_a = 0$, 1 in the (001) state. Additionally we have observed the transitions with $K_a = 4$ in the ground (000) state and with $K_a = 3$ and 4 in the (100) state and some transitions in the higher vibrational states. Assignment of transitions with $K_a \geqslant 3$ was made with both a line intensity analysis and a prediction of their frequencies from microwave data [12]. Measured frequencies of spectral lines included in the fitting procedure are given in Tables 1 and 2 for the ground (000) and the (100) exited vibrational states correspondingly.

In the course of the fit it turned out that it was necessary to review the assignment of some spectral series of $H_2O\cdots HF$ dimer observed in [12]. As it was mentioned above, we observed, in particular, lines with $K_a = 2$ and 3 in the lowest vibrational (100) state. Examining the recorded spectrum of $H_2O\cdots HF$ dimer we discovered that the branch of transitions with $K_a = 2$ following the series from [12] had much weaker intensity and the branch with $K_a = 3$ following the series from [12] had significantly greater intensity than it should be from comparative statistical weights of these states. This discrepancy between the observed intensities and the calculated ones led us to an idea that the transitions, identified in [12] as $K_a = 3$ branch, was actually the $K_a = 2$ branch. An independent check of this idea could be the observation of, for example, $K_a = 2$ line doubling. But in the frequency range up to 250 GHz (which was the highest frequency at the beginning of this study) such splitting had not been observed, because its value of 15 MHz at $J = 17$ (estimated from the asymmetry parameter $B - C$ of the order of 100 MHz) is less than a width of the lines. For this reason the research frequency range was extended up to 350 GHz and the splitting of the lines supposedly identified by us as a branch of rotational transitions with $K_a = 2$ was observed. The value of the splitting coincided with the predicted one, based on the known difference $B - C$ of the rotational constants of $H_2O\cdots HF$ dimer. Thus there were already two experimental facts in favor of our idea (line intensities and a doublet splitting of the lines, characteristic for transitions with $K_a = 2$) so we changed the assignment of the observed lines. The results of the fit with a new assignment are given in the Tables 1 and 2 for the (000) and (100) vibrational states, respectively.

In order to fit all available experimental data for the (000) and (100) vibrational states, we used the effective rotational Hamiltonian analogous to the one proposed by Watson [16]:

$$H = \left(A - \frac{B+C}{2}\right)J_z^2 + \frac{B+C}{2}J^2 + \left(\frac{B-C}{2} + 2d_J J^2\right)(J_x^2 - J_y^2) - D_J J^4 - D_{JK} J^2 J_z^2 + H_J J^6 + H_{JK} J^4 J_z^2 + H_{KJ} J^2 J_z^4$$

As it can be seen from the analysis of observed and calculated frequency differences in the column III of Tables 1

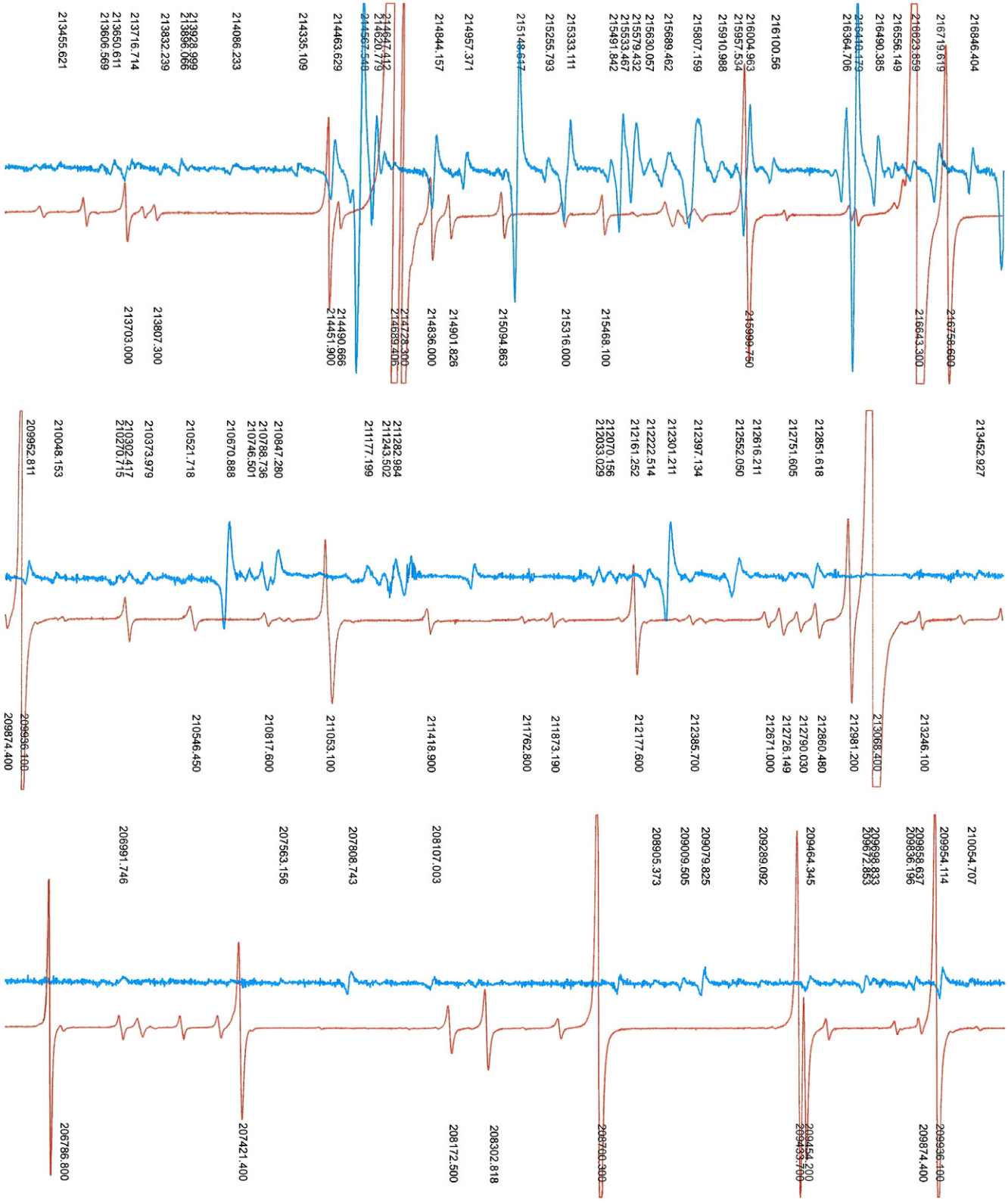

Fig. 2. Three fragments of $H_2O\cdots HF$ dimer spectrum (upper traces) recorded by the RAD-3 spectrometer simultaneously with SO_2 reference spectrum (lower traces). Measured frequencies of the studied spectrum and tabulated frequencies of the reference spectrum [14] are shown next to observed lines.

and 2 this Hamiltonian is not satisfactory and should be improved. This has been done in the present work by the following way.

It was mentioned in [12] that Coriolis interaction might take place between the ground and the first excited (100) vibrational states due to a quite small vibrational frequency

Table 1
Frequencies of transitions in MHz observed in this present work together with observed frequencies from ref. [12], identification of the transitions and differences between observed and calculated frequencies for (000) vibrational state of $H_2O\cdots HF$

Upper $J_{k_a k_c}$	Lower $J_{k_a k_c}$	Observed frequencies	Obs. − Calc. (MHz)			
			I	II	III	IV
1 0 1	0 0 0	14403.1	−0.2	0.2	0.7	0.2
2 0 2	1 0 1	28804.9	−0.7	−0.1	1.0	0.1
2 1 2	1 1 1	28673.4	0.6	0.0	−0.4	0.1
2 1 1	1 1 0	28920.5	0.3	−0.2	−0.7	−0.3
3 0 3	2 0 2	43205.5	−0.7	0.3	1.9	0.5
3 1 3	2 1 2	43007.7	0.6	−0.2	−0.8	−0.1
3 1 2	2 1 1	43379.0	0.9	0.1	−0.6	0.0
3 2 2	2 2 1	43159.2[a]	−0.9	−0.9	−6.6	−1.4
3 2 1	2 2 0	43159.2[a]				
4 0 4	3 0 3	57602.7	−1.5	−0.1	2.2	0.3
4 1 4	3 1 3	57340.0	1.3	0.2	−0.6	0.3
4 1 3	3 1 2	57834.7	1.3	0.2	−0.5	0.2
4 2 3	3 2 2	57542.5[a]	−0.4	−0.3	−7.9	−0.9
4 2 2	3 2 1	57542.5[a]				
4 3 2	3 3 1	57491.6	0.4	0.1	1.1	−0.7
5 0 5	4 0 4	71996.3	−2.3	−0.5	2.5	0.1
5 1 5	4 1 4	71668.5	1.6	0.3	−0.6	0.4
5 1 4	4 1 3	72286.8	1.5	0.2	−0.4	0.4
5 2 4	4 2 3	71921.6[a]	−0.6	−0.5	−9.8	−1.2
5 2 3	4 2 2	71921.6[a]				
5 3 3	4 3 2	71858.0	0.0	0.0	1.4	−0.9
13 0 13	12 0 12	186905.0			6.9	−0.9
13 1 13	12 1 12	186062.7			−2.7	−1.7
13 1 12	12 1 11	187664.1			0.1	0.7
13 2 12	12 2 11	186728.0[a]			−21.7	−1.3
13 2 11	12 2 10	186728.0[a]				
13 3 11	12 3 10	188564.0			8.8	−0.4
13 4 10	12 4 9	186300.8			−5.3	−0.1
14 0 14	13 0 13	201225.9			8.7	0.1
14 1 14	13 1 13	200322.3			−0.5	0.4
14 1 13	13 1 12	202043.1			0.5	1.0
14 2 13	13 2 12	201033.6[a]			−26.6	−4.9
14 2 12	13 2 11	201033.6[a]				
14 3 12	13 3 11	200864.9			14.2	3.8
14 4 11	13 4 10	200581.0			−1.8	3.2
15 0 15	14 0 14	215533.2			9.7	4.0
15 1 15	14 1 14	214569.2			1.4	2.1
15 1 14	14 1 13	216410.2			1.6	2.1
15 2 14	14 2 13	215333.1			−25.3	−2.2
15 2 13	14 2 12	215333.1				
15 3 13	14 3 12	215148.6			14.7	2.9
15 4 12	14 4 11	214844.2			−3.3	1.5
16 0 16	15 0 15	229826.2			10.1	0.1
16 1 16	15 1 15	228802.5			2.8	3.5
16 1 15	15 1 14	230760.7			−0.2	0.2
16 2 15	15 2 14	229613.0[a]			−30.1	−6.1
16 2 14	15 2 13	229613.0[a]				
16 3 14	15 3 13	229420.3			16.2	3.1
16 4 13	15 4 12	229099.8			0.1	5.2
17 0 17	16 0 16	244102.3			8.3	−2.4
17 1 17	16 1 16	243013.6			−3.9	−3.3
17 1 16	16 1 15	245097.1			−1.7	−1.3
17 2 16	16 2 15	243886.0[a]			−28.7	−2.9
17 2 15	16 2 14	243886.0[a]				
17 3 15	16 3 13	243679.8			19.4	5.1
17 4 14	16 4 12	243332.4			−4.7	−0.3
18 0 18	17 0 17	258370.7			14.2	3.1
18 1 18	17 1 17	257219.3			−1.1	−0.4
18 1 17	17 1 16	259417.9			−3.4	−2.8
18 2 17	17 2 16	258138.3[a]			−32.3	−5.1

(*continued on next page*)

Table 1 (*continued*)

Upper $J_{k_a k_c}$	Lower $J_{k_a k_c}$	Observed frequencies	Obs. − Calc. (MHz)			
			I	II	III	IV
18 2 16	17 2 15	258138.3[a]				
18 3 16	17 3 15	257918.1			16.2	−0.6
18 4 15	17 4 14	257554.9			−5.3	−1.3
19 0 19	18 0 18	272610.3			7.9	−3.7
19 1 19	18 1 18	271405.8			−1.7	−0.8
19 1 18	18 1 17	273727.4			0.0	0.7
19 2 18	18 2 17	272365.4			−29.9	−1.1
19 2 17	18 2 16	272388.2			−40.1	−11.3
19 3 17	18 3 16	272148.7			21.1	4.2
19 4 16	18 4 15	271765.1			−1.7	2.0
20 0 20	19 0 19	286841.3			10.2	−1.5
20 1 20	19 1 19	285574.9			−3.0	−1.8
20 1 19	19 1 18	288017.5			1.1	2.3
20 2 19	19 2 18	286583.2			−33.5	−3.0
20 2 18	19 2 17	286614.7			−40.4	−10.0
20 3 18	19 3 17	286356.5			19.7	1.6
20 4 17	19 4 16	285951.7			−7.3	−3.8
21 0 21	20 0 20	301055.9			14.5	2.8
21 1 21	20 1 20	299728.9			−1.9	−0.1
21 1 20	20 1 19	302288.2			0.9	2.8
21 2 20	20 2 19	300787.6			−32.8	−0.5
21 2 19	20 2 18	300826.9			−37.9	−5.6
21 3 19	20 3 18	300553.4			24.8	5.6
21 4 18	20 4 17	300129.9			−3.0	0.4
22 0 22	21 0 21	315244.8			12.2	0.8
22 1 22	21 1 21	313863.2			−2.0	0.5
22 1 21	21 1 20	316537.9			−1.3	1.5
22 2 21	21 2 20	314966.5			−39.1	−4.6
22 2 20	21 2 19	315014.5			−42.0	−7.5
22 3 20	21 3 19	314726.9			24.8	4.7
22 4 19	21 4 18	314284.0			−4.7	−1.2
23 0 23	22 0 22	329411.1			7.4	−3.4
23 1 23	22 1 22	327980.6			0.3	3.9
23 1 22	22 1 21	330767.2			−4.0	0.1
23 2 22	22 2 21	329127.3			−43.9	−7.0
23 2 21	22 2 20	329179.7			−49.8	−12.7
23 3 21	22 3 20	328875.7			19.3	−1.5
23 4 20	22 4 19	328415.5			−10.0	−6.2
24 0 24	23 0 23	343564.6			10.8	1.0
24 1 24	23 1 23	342071.3			−3.9	1.2
24 1 23	23 1 22	344979.6			−2.8	2.9
24 2 23	23 2 22	343277.8			−38.7	1.0
24 2 22	23 2 21	343335.1			−47.2	−7.6
24 3 22	23 3 21	343017.4			26.7	5.3
24 4 21	23 4 20	342536.9			−5.5	−1.2

[a] Central frequency of non–resolved doublet and differences between its experimental and calculated values.

of (100) mode equal to $64 \pm 10\ \mathrm{cm}^{-1}$. This interaction should affects, first of all, the energy levels with $K_a = 3$ in (000) and $K_a = 2$ in (100) states. But taking into account the Coriolis interaction in [12] only worsened the fit result and it was not clear whether the interaction took place.

The fit of the $H_2O\cdots HF$ spectrum data that we performed taking into account the Coriolis effect improved the discrepancy by almost a factor of 4. Contrary to [12], we took into account the Coriolis interaction not by exact diagnalization of the vibration–rotation matrix, but only approximately—we took into account only the main contributions to the most strongly interacting energy levels. Therefore, for the calculation of the energy levels with $K_a = 3$ (000) and $K_a = 2$, (100) we added in the Hamiltonian the term $a_1 J(J+1) + a_2 J^2(J+1)^2$ with a positive and the same term with a negative sign, respectively. Since *A*-constants are known only from *ab-initio* calculations, the $A - (B + C)/2$ values in this fit (and in all other fits we performed) were fixed to 390 and 360 GHz for the ground and (100) vibrational states respectively.

Along with the measured frequencies of $H_2O\cdots HF$ dimer, Tables 1 and 2 present in the Obs. – Calc. column following: (I) the result of the fit from [12]; (II) our fit of data [12] using the Hamiltonian as in [12] but taking into account our reassignment of the transitions; (III) the fit of all available data without taking into account the

Table 2
Frequencies of transitions in MHz observed in this work together with observed frequencies from ref. [12], identification of the transitions and differences between observed and calculated frequencies for (100) vibrational state of $H_2O\cdots HF$

Upper $J_{k_a k_c}$	Lower $J_{k_a k_c}$	Observed frequencies[a]	Obs. − Calc. (MHz)			
			I	II	III	IV
1 0 1	0 0 0	14517.2	0.2	−0.1	−0.4	−0.4
2 0 2	1 0 1	29033.3	0.1	−0.4	−1.1	−1.0
2 1 2	1 1 1	28930.5	0.8	0.6	1.1	1.0
2 1 1	1 1 0	29121.0	−1.1	−1.3	−0.9	−0.9
3 0 3	2 0 2	43548.2	0.5	0.0	−1.1	−0.9
3 1 3	2 1 2	43392.0	−0.5	−0.6	0.1	0.0
3 1 2	2 1 1	43682.6	1.6	1.5	2.1	2.0
4 0 4	3 0 3	58060.3	0.7	0.3	−1.3	0.9
4 1 4	3 1 3	57853.1	0.4	0.5	1.3	1.2
4 1 3	3 1 2	58236.7	−0.7	−0.6	0.2	0.1
4 2 3	3 2 2	57982.2[b]		0.0	−11.4	0.2
4 2 2	3 2 1	57932.2[b]				
5 0 5	4 0 4	72568.0	−0.2	−0.1	−2.2	−1.7
5 1 5	4 1 4	72308.7	−0.9	−0.3	0.5	0.4
5 1 4	4 1 3	72789.9	−0.5	0.1	1.0	1.0
13 0 13	12 0 12	188387.5			13.6	−10.2
13 1 13	12 1 12	187734.8			6.0	8.0
13 1 12	12 1 11	188968.7			−1.0	0.9
13 2 12	12 2 11	188148.1[b]			−40.4	0.3
13 2 11	12 2 10	188148.1[b]				
13 3 11	12 3 10	187931.5			−18.5	−5.6
13 4 10	12 4 9	187619.9			−2.5	−2.3
14 0 14	13 0 13	202827.4			−9.1	−5.1
14 1 14	13 1 13	202115.2			0.9	3.4
14 1 13	13 1 12	203447.6			−1.3	1.1
14 2 13	13 2 12	202565.2[b]			−44.0	−0.5
14 2 12	13 2 11	202565.2[b]				
14 3 12	13 3 11	202328.7			−5.4	−9.3
14 4 11	13 4 10	202000.4			1.3	1.4
15 0 15	14 0 14	217249.8			−9.5	−4.8
15 1 15	14 1 14	216490.4			2.9	5.9
15 1 14	14 1 13	217914.4			−1.0	1.9
15 2 14	14 2 13	216970.6[b]			−46.9	0.2
15 2 13	14 2 12	216970.6[b]				
15 3 13	14 3 12	216719.6			−2.9	−7.0
15 4 12	14 4 11	216364.7			1.2	1.3
16 0 16	15 0 15	231665.0			−3.5	2.0
16 1 16	15 1 15	230849.7			2.1	5.8
16 1 15	15 1 14	232371.7			3.4	6.9
16 2 15	15 2 14	231363.2[b]			−49.4	1.3
16 2 14	15 2 13	231363.2[b]				
16 3 14	15 3 13	231095.0			−2.6	−6.7
16 4 13	15 4 12	230714.0			−0.5	−0.5
17 0 17	16 0 16	246052.0			−11.2	−4.9
17 1 17	16 1 16	245202.0			8.4	12.8
17 1 16	16 1 15	246808.2			1.5	5.6
17 2 16	16 2 15	245744.6[b]			−48.9	5.5
17 2 15	16 2 14	245744.6[b]				
17 3 15	16 3 13	245457.6			−0.8	−5.1
17 4 14	16 4 12	245060.0			8.8	8.6
18 0 18	17 0 17	260431.5			−10.9	−3.7
18 1 18	17 1 17	259522.7			−1.9	3.2
18 1 17	17 1 16	261231.3			1.7	6.5
18 2 17	17 2 16	260103.2[b]			−56.2	1.9
18 2 16	17 2 15	260103.2[b]				
18 3 16	17 3 15	259811.3			7.1	2.7
18 4 15	17 4 14	259369.9			−2.9	−3.3
19 0 19	18 0 18	274793.3			−11.9	−3.8
19 1 19	18 1 18	273840.5			0.8	6.7
19 1 18	18 1 17	275641.6			5.4	11.0

Table 2 (*continued*)

Upper $J_{k_a k_c}$	Lower $J_{k_a k_c}$	Observed frequencies[a]	Obs. − Calc. (MHz)			
			I	II	III	IV
19 2 18	18 2 17	274452.7[b]			−56.7	5.2
19 2 17	18 2 16	274452.7[b]				
19 3 17	18 3 16	274128.7			−5.2	−9.8
19 4 16	18 4 15	273681.8			3.4	2.8
20 0 20	19 0 19	289136.9			−13.9	−4.8
20 1 20	19 1 19	288132.9			−5.1	1.6
20 1 19	19 1 18	290026.7			1.3	7.6
20 2 19	19 2 18	288769.1			−60.9	4.8
20 2 18	19 2 17	288790.9			−64.1	1.6
20 3 18	19 3 17	288442.9			−3.8	−8.6
20 4 17	19 4 16	287972.4			5.4	4.4
21 0 21	20 0 20	303461.5			−16.6	−6.5
21 1 21	20 1 20	302421.1			2.4	9.9
21 1 20	20 1 19	304394.0			−2.4	4.7
21 2 20	20 2 19	303078.1			−65.3	4.3
21 2 19	20 2 18	303106.7			−65.6	4.0
21 3 19	20 3 18	302744.6			2.9	−2.1
21 4 18	20 4 17	302243.8			6.0	4.6
22 0 22	21 0 21	317767.2			−19.1	−7.9
22 1 22	21 1 21	316678.1			−2.7	5.7
22 1 21	21 1 20	318740.7			−7.5	0.4
22 2 21	21 2 20	317369.0			−68.9	4.5
22 2 20	21 2 19	317403.7			−67.4	6.1
22 3 20	21 3 19	317016.8			−1.0	−6.3
22 4 19	21 4 18	316496.3			6.6	4.6
23 0 23	22 0 22	332052.0			−22.3	−10.2
23 1 23	22 1 22	330917.7			−5.6	3.6
23 1 22	22 1 21	333073.7			−6.1	2.6
23 2 22	22 2 21	331643.1			−69.6	7.8
23 2 21	22 2 20	331680.2			−70.2	7.1
23 3 21	22 3 20	331275.6			1.3	−4.4
24 0 24	23 0 23	346319.1			−22.3	−9.1
24 1 24	23 1 23	345139.4			−6.1	4.0
24 1 23	23 1 22	347385.8			−4.6	4.8
24 2 23	23 2 22	345891.5			−75.2	6.0
24 2 22	23 2 21	345937.1			−72.4	8.8
24 3 22	23 3 21	345511.7			1.5	−4.7

[a] Data from work [12] having incorrect identification and thus producing largest in [12] Obs. − Calc. differences are not presented in the table.
[b] Central frequency of non–resolved doublet and differences between its experimental and calculated values.

Coriolis interaction; (IV) fit of all data with taking into account the effect of Coriolis interaction. The final fit residuals are still somewhat larger than an estimated experimental error. The most probable reason is an accidental overlapping of broad lines in a very dense spectrum of $H_2O\cdots HF$ dimer, observed with a static pressure gas phase cell, as it can be seen from Fig. 2. Tables 3 and 4 give the rotational, centrifugal distortion and Coriolis interaction constants, obtained from the fits described above for the (000) and (100) vibrational states, respectively.

Table 3
Fitted Hamiltonian constants of (000) state of $H_2O\cdots HF$

		I	II	III
$(B+C)/2$	MHz	7201.54(2)	7201.283(8)	7201.510(8)
$(B-C)/2$	MHz	61.84(2)	61.87(2)	69.89(2)
D_J	kHz	35.9(5)	36.95(3)	36.63(3)
D_{JK}	MHz	2.02(1)	1.620(2)	1.976(2)
d_J	kHz		0.56(1)	0.58(1)
H_J	mHz		21(34)	−366(34)
H_{JK}	Hz		52(2)	68(2)
H_{KJ}	kHz	32(1)	9.5(1)	29.5(1)
a_1	MHz	1.6		1.57
a_2	kHz			0.08

We would like to make some remarks concerning the observed in the present work lines, which were not included in the fits. The spectral lines of the transitions with $K_a = 5$ in both the (000) and (100) states appear to overlap with the $K_a = 1$ lines. These lines begin to be resolved only at $J \sim 20$. The lines with higher values of K_a have small intensity due to the Boltzmann factor and it is difficult to identify them unambiguously among other weak lines. This also concerns lines corresponding to higher vibrational states. Nevertheless we were able to find some series of lines that could be preliminarily identified as rotational transitions of $H_2O\cdots HF$ dimer in the (200), (101) and (011) states, which have not been studied before. However,

Table 4
Fitted Hamiltonian constants of (100) states of $H_2O\cdots HF$

		I	II	III
$(B+C)/2$	MHz	7258.73(4)	7258.938(9)	7258.864(9)
$(B-C)/2$	MHz	48.09(3)	48.12(2)	48.12(2)
D_J	kHz	37.6(8)	37.21(5)	37.04(5)
D_{JK}	MHz	1.85(3)	2.332(6)	2.160(6)
d_J	kHz		0.58(2)	0.58(2)
H_J	mHz		−27(70)	−130(70)
H_{JK}	Hz		58(5)	13(5)
H_{KJ}	kHz	−47(10)	26.4(3)	17.1(3)
a_1	MHz	−1.6		−1.57
a_2	kHz			−0.08

doubtless identification of these series requires further experimental and theoretical studies and goes out of the frame of this publication. We do not present here the result of analysis of lines in the (010) and (001) vibrational states because the number of unambiguously identified lines in these states and a relatively large uncertainty of their measured frequencies did not allow us to improve the constants known from [12]. We found also some series of lines, which do not belong to the pure rotational spectrum of $H_2O\cdots HF$ dimer in the studied configuration. Further identification of observed lines meets serious difficulties at our level of understanding of the dimer spectrum but it could be the subject of future publications, if an appropriate *ab-initio* calculation will be made.

In summary, this study of the spectrum of the $H_2O\cdots HF$ dimer in short millimeter- and long submillimeter-wave ranges has considerably expanded the amount of available experimental data, including a new data on the excited vibrational states of the dimer. The assignment of spectral line series observed earlier with a microwave spectrometer has been corrected on the basis of new experimental submillimeter-wave data. The data on Coriolis interaction of the energy levels of the ground and the first excited vibrational states of the H_2O–HF dimer have been obtained. The effective rotational molecular constants of the $H_2O\cdots HF$ complex in (000) and (100) vibrational states have been essentially refined.

Acknowledgments

Authors thank S.E. Tretyakova for her great help with the paper artwork. The work was partly supported through RFBR Grant No 06-02-16082-a.

Appendix A

The RAD-3 spectrometer was first reported at the Prague meeting in 1986 [13]. Later it was successfully used for study of submillimeter-wave spectra of the acetaldehyde (CH_3CHO) [17,18], methyl fluoride (CH_3F) [19,20], hydrogen selenid (H_2Se) [21,22], hydrogen fluoride dimer ($HF\cdots HF$) [7] and $H_2O\cdots HF$ dimer [23]. These publications did show the advantages of this simple BWO-based spectrometer with a continuous broad band frequency scanning capability and automated line frequency measurements for an investigation of dense molecular spectra such as spectrum of the acetaldehyde molecule [17,18]. The main ideas of this spectrometer led later to the successful development of FASSST BWO-based spectrometer [24,25]. However, a description of the RAD-3 spectrometer was not reported in any widely available publication in English except a short paragraph in a review paper [26]. Using the opportunity we present here the main principals of operation and technical parameters of the RAD-3 spectrometer.

The RAD-3 spectrometer (Fig. 1) represents well known RAD spectrometer [8] additionally equipped with: (1) the system of BWO frequency stabilization against tunable Fabry–Perot cavity; (2) computer interface and (3) the corresponding software for an automated: (i) detection of all lines in the recorded spectra with an amplitude exceeding the preset threshold level, (ii) assignment of the reference spectrum lines, and (iii) calculation of the frequency of all detected lines in a studied spectrum.

The RAD-3 spectrometer (Fig. 1) employs the Istok's BWOs as a broad band electronically tunable source of coherent submillimeter-wave radiation. A minor part (10–20%) of the BWO radiation is split and used for BWO frequency stabilization. The main part of the radiation is directed into two static pressure gas cells with build-in capacitance microphones for a radio acoustical detection of the gas absorption. One cell is filled by the investigated gas and the other one by the reference gas with known spectrum. The cells are equipped with high sensitive capacitance sensors (CS) transforming the microphone signal into electrical signal. The CS output signals are digitized by two-channel digital lock-in amplifier board and recorded into computer.

Frequency of the BWO radiation is stabilized against a resonance frequency of Fabry–Perot cavity mode as described in [27,28]. Quality of the Fabry–Perot cavity is made so the width of its resonance roughly corresponded to the width of molecular spectral lines and thus a deviation of BWO frequency modulation employed in the spectrometer is optimal for both the spectral lines and the Fabry–Perot cavity resonance observation. The lock-in amplifier in the BWO frequency lock-in loop operates in one-F mode with a time constant of ~0.6 s. Output signal of this amplifier is used as the BWO frequency control voltage. DC part of the control voltage drives a regulator of the BWO high voltage power supply thus the stabilized BWO can be tuned over its entire frequency range.

The BWO radiation frequency scanning is performed by a smooth mechanical move of one of the Fabry–Perot cavity mirror. It's known that the resonance frequency of the cavity is changed according to the equation $\Delta f = f \cdot \Delta L/L$, where f is the eigenmode frequency; L is the cavity length and Δf and ΔL are increments of these parameters. The BWO radiation frequency locked to the cavity resonance follows the same rule. ΔL value in the RAD-3 spectrometer is measured by Michelson interferometer

fed by highly stable (relative frequency instability $\sim 10^{-8}$) single mode red light He–Ne laser. While the cavity length is smoothly tuned the interferometer output signal is recorded simultaneously with lines of studied and reference molecular spectra as it is shown in the left part of Fig. 3. Line positions in the recorded spectra can be determined relatively to interferometer fringes with an uncertainty of 0.01 fraction of its period or ~6 kHz. It allows to calculate accurately from the tabulated frequencies of two observed reference lines both an effective value of L and a BWO frequency change corresponding to one period of the interferogram. Since L is permanently changing in course of the spectrum record, the absolute frequency for each given point n of the recorded spectra is given by the equation:

$$f(n) = f_1 \cdot \left(1 - \frac{n - n_1}{n_2 - n_1} \cdot \frac{f_2 - f_1}{f_2}\right)^{-1}, \quad (1)$$

where f_1 and f_2 are the reference line tabulated frequencies; $(n_2–n_1)$ is decimal number of the interferogram periods between these reference lines; n is the position of a given point in the interferogram period decimal number. Eq. (1) allows an accurate interpolation of BWO radiation frequency between the reference lines. It is also used for prediction of the position of a "next" reference line in the algorithm of an automated assignment of the reference spectrum lines. If there is no line within the predicted position uncertainty or there is a line but its amplitude does not match the tabulated intensity of the transition, the algorithm tries the next line from the reference spectrum catalog. The algorithm is very robust, reliable and works well even when some of weak reference spectrum lines are not seen in observed spectrum or/and the reference spectrum is "polluted" by lines of other molecules (e.g. H_2O) not included in the catalog. However, the frequency of the very first reference line in the recorded spectrum should be manually indicated by operator. In RAD-3 it can be done easy because the absolute frequency of the line can be estimated using a mode of operation when BWO is stabilized against the reference line center and the Fabry–Perot cavity serves as a wave-meter.

Right side of Fig. 3 demonstrates stability of BWO frequency locked to the cavity eigenmode. After two reference lines were recorded (left part of Fig. 3) the movable mirror of the cavity was stopped and returned back to the position where the BWO frequency corresponds to some point at the slope of the second reference line. Then the mirror position was stable for some time, as confirmed by stable level of the interferometer output signal. The BWO frequency fluctuations were transformed by the line slope into the absorption signal amplitude fluctuations. These fluctuations are shown in Fig. 3 magnified by 20-X. Known width of the reference line (~12 MHz) lets us to estimate the magnitude of frequency deviations of locked BWO as not exceeding 50 kHz.

The accuracy of frequency measurements with RAD-3 spectrometer was calibrated using frequency synthesizer. In this experiment the phase locked to a harmonic of the microwave frequency synthesizer BWO was also locked to the Fabry–Perot cavity resonance as described above except the control voltage of the second lock-in loop was applied not to the BWO power supply but to the microwave synthesizer input. Thus the cavity was a master and synthesizer was a slave. In a course of the experiment the Fabry–Perot cavity mirror was slowly moved and both output signal of the Michelson interferometer as well as the synthesizer frequency were recorded to the computer. The absolute frequencies of the BWO radiation corresponding to the first and last points of the recorded file were used as the tabulated frequencies f_1 and f_2 in Eq. (1). The frequencies of all other points were automatically calculated by the computer and then compared with the BWO absolute frequencies. The results of the comparison are shown in Fig. 4. Upper plot in Fig. 4 corresponds to

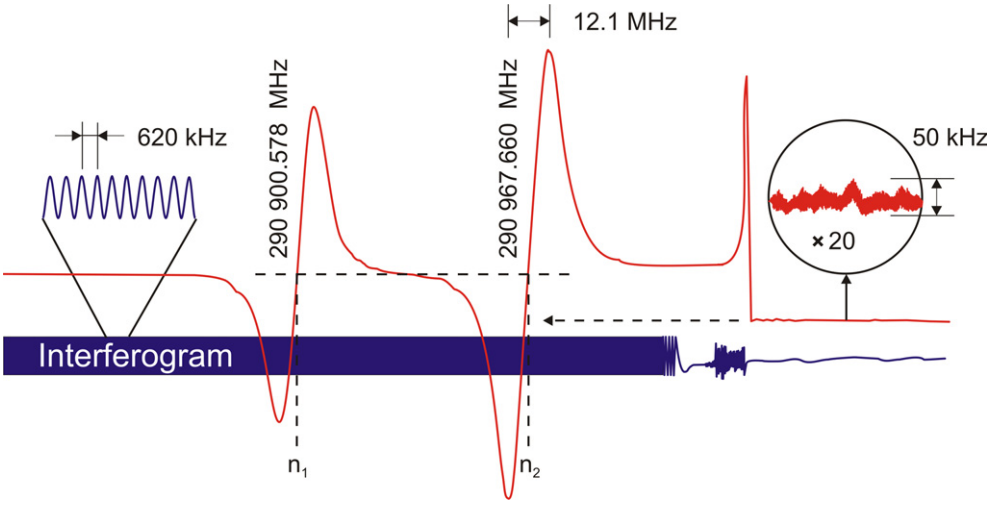

Fig. 3. Example of record of molecular spectral lines together with interferogram in the RAD-3 spectrometer and demonstration of radiation frequency stability in the spectrometer at the spectral line slope (right part of the figure). See appendix text for details.

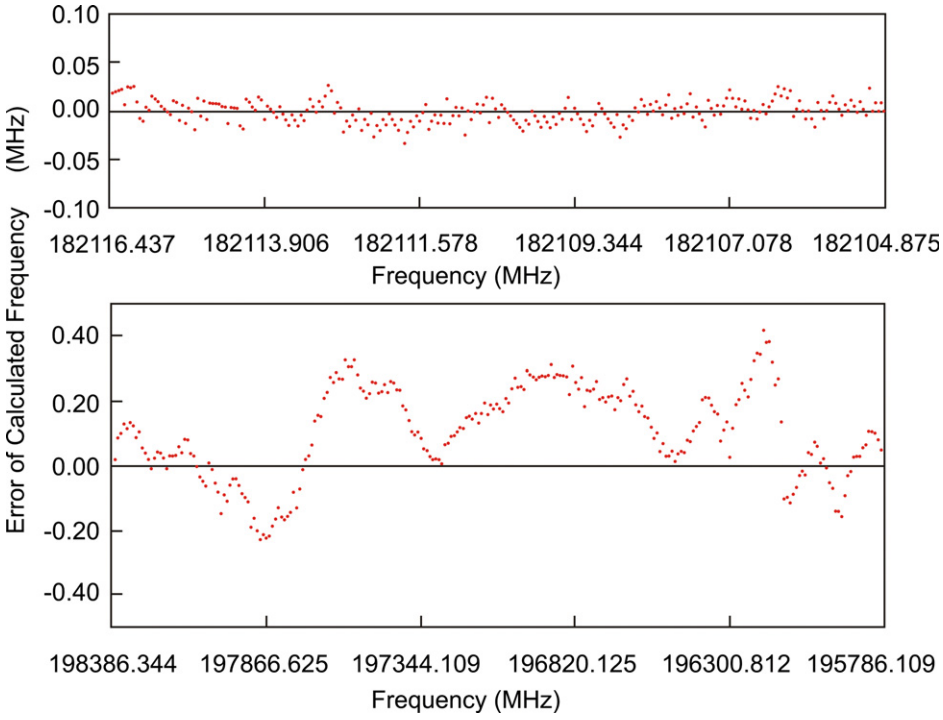

Fig. 4. Calibration of accuracy of frequency measurements in the RAD-3 spectrometer performed using frequency synthesizer. Differences between absolute radiation frequency determined by the synthesizer and one measured by the RAD-3 spectrometer are plotted versus frequency for narrow (~11.5 MHz) and wide (~2.6 GHz) frequency scans shown in upper and lower parts of the plot correspondingly. See appendix text for details.

narrow frequency scan of about 11.5 MHz. One can see that uncertainty of the frequency measurements with the RAD-3 within such narrow range is practically free from systematical errors and remains within ±20 kHz. This value corresponds well to the frequency fluctuations measurements (Fig. 3). Such high accuracy of frequency measurements with RAD-3 allows its use for studies of molecular line shape parameters including the line pressure shift and pressure broadening. However in a broad band scan the uncertainty of RAD-3 frequency measurement is increased up to about ±300 kHz as it is seen from the lower plot in Fig. 4. The uncertainty increase is most likely related to a small systematical distortion in the cavity resonance response shape due to radiation interference effects and a multimode structure of BWO radiation. The scan width in the second case (~2.6 GHz) was a few times wider than the average distance between SO_2 molecule spectral lines used as reference spectrum.

It is known that molecular line recorded with use of lock-in amplifier has a little frequency shift due to a time constant. This shift does not affect an accuracy of measurements with RAD-3 spectrometer because it is the same for the lines of investigated and reference spectra if they have the same line width.

Finally uncertainty of frequency measurements with the RAD-3 spectrometer was obtained in a series of measurements of strong isolated SO_2 spectral lines whose frequencies were excluded from the reference lines catalog and the lines were considered as studied lines. In these measurements the deviation of measured frequency from its tabulated value [14] was not exceeding ±500 kHz.

Thus broad band spectra with a great number of lines can be measured with RAD-3 spectrometer with rather good accuracy and listed practically automatically.

References

[1] W. Klemperer, J. Mol. Struct. 59 (1980) 161–176.
[2] A.G. Legon, D.J. Millen, Chem. Rev. 86 (1986) 635–657.
[3] B.M. Smirnov, Usp. Fiz. Nauk+. 142 (1) (1984) 31–60.
[4] A.A. Vigasin, In: "Microwave Spectroscopy and Its Application", collected papers of the Council of the USSR Academy of Sciences on Spectroscopy, M., (1985) 6-64.
[5] W.J. Lafferty, R.D. Suenram, F.J. Lovas, J. Mol. Spectrosc. 123 (1987) 434–452.
[6] N.F. Zobov, E.N. Karyakin, Izv. Vuz. Radiofiz+. (in Russian, available in English translation as Radiophysics and Quantum Electronics), 31 (11) (1988) 1415–1417.
[7] S.P. Belov, E.N. Karyakin, I.N. Kozin, A.F. Krupnov, O.L. Polyansky, M.Yu. Tretyakov, N.F. Zobov, R.D. Suenram, W.J. Lafferty, J. Mol. Spectrosc. 141 (1990) 204–222.
[8] A.F. Krupnov, A.V. Burenin, New Methods in Submillimeter Microwave Spectroscopy, in: K.N. Rao (Ed.), Molecular Spectroscopy: Modern Research, Academic Press, N.Y, 1976, pp. 93–126.
[9] J.W. Bevan, A.C. Legon, D.J. Millen, S. Rogers, J. Chem. Soc. Chem. Commun. (1975) 341.
[10] J.W. Bevan, Z. Kisiel, A.C. Legon, D.J. Millen, S.C. Rogers, Proc. Roy. Soc. A372 (1980) 441.
[11] Z. Kisiel, A.C. Legon, D.J. Millen, Proc. Roy. Soc. A381 (1982) 419.
[12] G. Gazzoli, P.G. Favero, D.G. Lister, A.C. Legon, D.J. Millen, Z. Kisiel, Chem. Phys. Lett. 117 (1985) 543–549.

[13] S.P. Belov, M.Yu. Tretyakov, in: Proceedings of the IXth International Conference on High Resolution, IR Spectroscopy, Prague, 1986, p. 68.
[14] S.P. Belov, M.Yu. Tretyakov, I.N. Kozin, E. Klisch, G. Winnewisser, J.-M. Flaud, W.J. Lafferty, J. Mol. Spectrosc. 191 (1998) 17–27.
[15] F.M. Rappoport, A.A. Il'inskaya, in: Goskhimizdat, M. (Ed.), Laboratory Methods of Pure gas Obtaining, 1963.
[16] J.K.G. Watson, J. Chem. Phys. 46 (1967) 1935–1949.
[17] S.P. Belov, M.Yu. Tretyakov, I. Kleiner, J.T. Hougen, J. Mol. Spectrosc. 160 (1993) 61–72.
[18] I. Kleiner, J.T. Hougen, J.-U. Grabov, S.P. Belov, M.Yu. Tretyakov, J. Cosleu, J. Mol. Spectrosc. 179 (1996) 41–60.
[19] S.P. Belov, M.Yu. Tretyakov, P. Pracna, D. Papousek, K. Sarka, J. Mol. Spectrosc. 146 (1) (1991) 120–126.
[20] S.P. Belov, M.Yu. Tretyakov, D. Papousek, P. Pracna, R. Tesar, J. Kauppinen, J. Mol. Spectrosc. 146 (1) (1991) 127–134.
[21] I.N. Kozin, S.P. Belov, O.L. Polyansky, M.Yu. Tretyakov, J. Mol. Spectrosc. 152 (1992) 13–28.
[22] M.Yu. Tretyakov, S.P. Belov, I.N. Kozin, O.L. Polyansky, J. Mol. Spectrosc. 154 (1992) 163–168.
[23] S.P. Belov, V.M. Demkin, N.F. Zobov, E.N. Karyakin, A.F. Krupnov, I.N. Kozin, O.L. Polyansky, M.Yu. Tretyakov, Preprint IAP RAS No. 192 (1988).
[24] D.T. Petkie, T.M. Goyette, R.P. Bettens, S.P. Belov, S. Albert, P. Helminger, F.C. De Lucia, Rev. Sci. Instrum. 68 (4) (1996) 1675–1682.
[25] S. Albert, D.T. Petkie, R.P.A. Bettens, S.P. Belov, F.C. De Lucia, Anal. Chem. 70 (21) (1998) 719A–727A.
[26] A.F. Krupnov, Spectrochim. Acta. A. 52 (1996) 967–993.
[27] Yu.A. Dryagin, A.F. Krupnov, V.A. Skvortsov, Pribori i Tekhika Eksperimenta (in Russian, available in English translation as Instrum. Exp. Tech.), 1, (1969) 95-99.
[28] S.P. Belov, L.I. Gershtein, E.N. Karyakin, A.F. Krupnov, Pribori i Tekhika Eksperimenta (in Russian, available in English translation as Instrum. Exp. Tech.), 3, (1973) 142-147.
[29] A.J. Sadlej, O. Bludsky, V. Spirko, Coll. Czech. Chem. Comm. 58 (12) (1993) 2813.
[30] V.P. Bulychev, E.I. Gromova, K.G. Tokhadze, Opt. Spectrosc. 96 (5) (2004) 774–780.
[31] V.P. Bulychev, I.M. Gregoriev, E.I. Gromova, K.G. Tokhadze, Phys. Chem. Chem. Phys. 7 (2005) 2266–2278.
[32] Zhenhong Yu, W. Klemperer, Proc. Natl. Acad. Sci. USA 102 (36) (2005) 12667–12669.
[33] Bruno Madebene, PhD Thesis "Etude théorique du couplage vibrationnel de la liaison hydrogène dans les complexes $HX\cdots H_2Y$ (X=F, Cl et Y=O, S)", Université Pierre et Marie Curie U.F.R. de Chimie, PARIS VI (2005).
[34] M. Lewerenz, private communication, 2006.